ICIC Express Letters
Volume **10**, Number **9**, September **2016**

ICIC International ©2016 ISSN 1881-803X
pp. 2197–2203

FREQUENCY STABILIZATION OF NONLINEAR RENEWABLE POWER SYSTEMS VIA SLIDING MODE AND NEURAL NETWORKS

Yan Ren[1,2], Yaxiong Bi[1], Chuanli Gong[3] and Dianwei Qian[4]

[1]China Three Gorges Corporation
No. 1, Yuyuantan South Road, Haidian District, Beijing 100038, P. R. China

[2]School of Electric Power
North China University of Water Resources and Electric Power
No. 36, Beihuan Road, Zhengzhou 450045, P. R. China

[3]Wuling Power Corporation
No. 188, Wuling Road, Changsha 410004, P. R. China

[4]School of Control and Computer Engineering
North China Electric Power University
No. 2, Beinong Road, Changping District, Beijing 102206, P. R. China
dianwei.qian@ncepu.edu.cn

Received January 2016; accepted April 2016

Abstract. *With the development of wind energy, its intermittency challenges frequency stabilization of power systems. Power systems also suffers from the nonlinearity of generation rate constraint (GRC). The intermittency and nonlinearity challenge load frequency control (LFC). This paper addresses a control scheme for the LFC problem of a nonlinear power system with wind turbines. To achieve the LFC task of the power system, the control scheme combines sliding mode control and neural networks. From the Lyapunov direct method, update formulas of the neural networks are formulated so that the control system is of asymptotic stability. Simulation results are presented to show the performance and effectiveness of the presented control scheme.*
Keywords: Load frequency control, Renewable power system, Neural networks

1. **Introduction.** Wind energy is now the fastest growing energy source around the world because of its zero emission [1]. The percentage of wind power in power systems increases with years [2]. Influenced by climate changes, the power output of wind power is random and intermittent, which would pose a reliability supply challenge [3].

Load frequency control (LFC) is a profitable auxiliary service to preserve the balance between power generation and power consumption [4]. Recently, advanced control methods have been applied to the LFC problem. Many previous reports [4, 5, 6, 7] only consider traditional power sources rather than renewable ones. With the increasing percentage of wind power, the LFC problem of power systems with wind turbines has been paid more and more attention.

Inherently, power systems are nonlinear [8]. The existence of the non-linearities in power systems deteriorates the system performance, and even affects the system stability. In order to solve the nonlinearity of generation rate constraint (GRC), a common approach is to design a controller for the linearized nominal model; then the controller is directly imposed on the original nonlinear system [6, 7]. To some extent, the common approach can work but has some potential hazards because of no theoretically guaranteed stability.

The methodology of RBF networks is a universal approximator [9]. So far, how to conquer the GRC nonlinearity by RBF networks remains untouched and problematic. This paper focuses on the SMC method for LFC of nonlinear power systems with wind turbines. Sliding-mode-based neural networks are designed to suppress the entire uncertainties. Some results are presented by a nonlinear power system with wind turbines.

2. **System Configuration.** Consider a multi-area interconnected power system. The power system is composed of N control areas which are interconnected by tie-lines. Figure 1 represents the block diagram of the ith control area. In Figure 1, variables $\Delta P_{gi}(t)$, $\Delta X_{gi}(t)$ and $\Delta f_i(t)$ are the incremental changes of generator output, governor valve position, and frequency, respectively. $\Delta P_{Li}(t)$ is load disturbance, and $\Delta P_{ci}(t)$ is control input. T_{gi}, T_{ti} and T_{pi} are the time constants of governor, turbine and electric system governor, respectively. $B_i = \frac{1}{R_i} + \frac{1}{K_{pi}}$ is the frequency bias factor where R_i is adjustment deviation coefficient and K_{pi} is electric system gain. T_{ij} is the synchronizing power coefficient between area i and area j, $i = 1, \ldots, N$ and N is the number of control areas.

The area control error (ACE) in the ith control area is defined by $ACE_i(t) = \Delta P_{tie,i}(t) + B_i \Delta f_i(t)$, where $\Delta P_{tie,i}(t)$ is the tie-line active power deviation. To force $ACE_i(t)$ to zero, the integral of $ACE_i(t)$, an additional state, is determined by $\Delta E_i(t) = K_{Ei} \int ACE_i(t) dt$, where K_{Ei} is the gain of this additional state.

Define $\mathbf{x}_i(t) = [\Delta X_{gi}(t)\ \Delta P_{gi}(t)\ \Delta f_i(t)\ \Delta P_{tie,i}(t)\ \Delta E_i(t)]^T$. Having linearized the GRC nonlinearity, the model, describing the LFC problem in Figure 1, is written by

$$\dot{\mathbf{x}}_i(t) = \mathbf{A}_i \mathbf{x}_i(t) + \mathbf{B}_i u_i(t) + \mathbf{F}_i \Delta \mathbf{P}_{di}(t) \tag{1}$$

where $u_i(t) = \Delta P_{ci}(t)$ is the control input, and $\Delta \mathbf{P}_{di}^T(t) = [\Delta P_{Li}(t)\quad \Delta V_i(t)]$. Concerning the nominal power system, $\mathbf{A}_i$, $\mathbf{B}_i$ and $\mathbf{F}_i$ are formulated by [3].

Mohamed and his colleagues [3] presented a simplified frequency response model of a DFIG-based wind turbine unit and the structure of the model is illustrated in Figure 2.

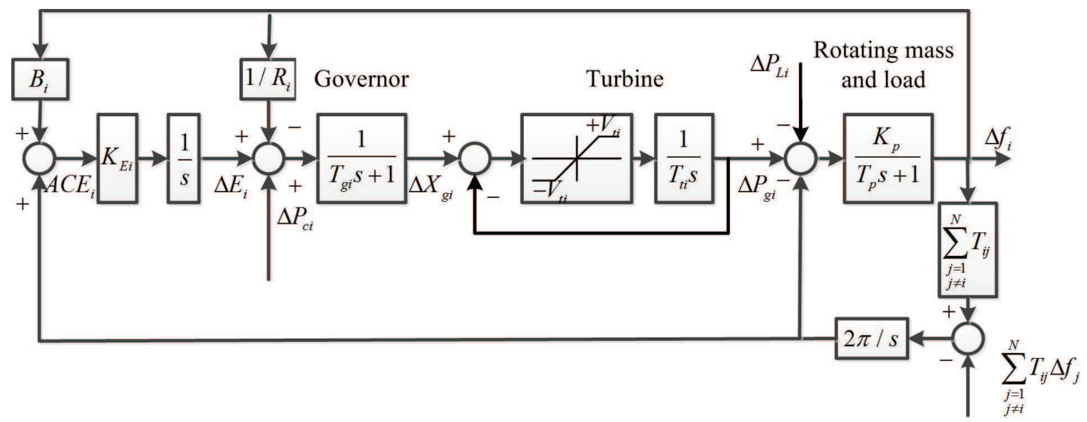

FIGURE 1. Dynamic model of the ith control area of the nonlinear power system

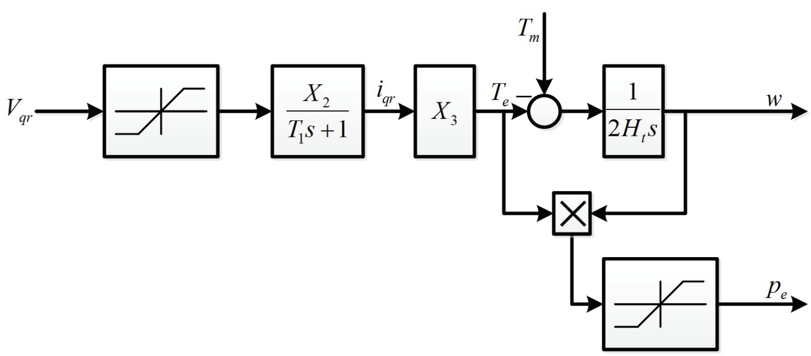

FIGURE 2. Simplified model of DFIG based wind turbine

The model in Figure 2 can be described by $\dot{i}_{qr}(t) = -\left(\frac{1}{T_1}\right) i_{qr}(t) + \left(\frac{X_2}{T_1}\right) V_{qr}(t)$, $\dot{w}(t) = -\left(\frac{X_3}{2H_t}\right) i_{qr}(t) + \left(\frac{1}{2H_t}\right) T_m(t)$ and $P_e(t) = w(t)X_3 i_{qr}(t)$, where $i_{qr}(t)$ is the q-axis component of the rotor current, $V_{qr}(t)$ is the q-axis component of the rotor voltage, $w(t)$ is the rotational speed, $T_m(t)$ is the mechanical power, H_t is the equivalent inertia constant of wind turbine and $P_e(t)$ is the active power of wind turbine. Other symbols are explained as $X_2 = \frac{1}{R_r}$, $X_3 = \frac{L_m}{L_{ss}}$, $T_1 = \frac{L_0}{w_s R_s}$, $L_0 = L_{rr} + \frac{L_m^2}{L_{ss}}$, $L_{ss} = L_s + L_m$ and $L_{rr} = L_r + L_m$, where L_m is the magnetizing inductance, R_r is the rotor resistance, R_s is the stator resistance, L_r is the rotor leakage inductance, L_s is the stator leakage inductance, L_{rr} is the rotor self-inductance, L_{ss} is the stator self-inductance and w_s is the synchronous speed.

Define $\mathbf{x}_{wi}(t) = [\Delta X_{gi}(t)\ \Delta P_{gi}(t)\ \Delta f_i(t)\ \Delta P_{tie,i}(t)\ \Delta i_{qr,i}(t)\ \Delta w_i(t)\ \Delta E_i(t)]^T$. Then, the mathematical model, describing the LFC problem in Figure 2, has a form of

$$\dot{\mathbf{x}}_{wi}(t) = \mathbf{A}_{wi}\mathbf{x}_{wi}(t) + \mathbf{B}_{wi}\mathbf{u}_{wi}(t) + \mathbf{F}_{wi}\Delta\mathbf{P}_{wdi}(t) \tag{2}$$

where $\mathbf{u}_{wi}^T(t) = [\Delta P_{ci}(t)\ \Delta V_{qr,i}(t)]$ and $\Delta\mathbf{P}_{wdi}^T(t) = [\Delta P_{Li}(t)\ \Delta V_i(t)\ \Delta T_{mi}(t)]$. Concerning the nominal power system, $\mathbf{A}_{wi}$, $\mathbf{B}_{wi}$ and $\mathbf{F}_{wi}$ are are formulated by [3].

From (1) and (2), both the system models can be described by a uniform expression. Without loss of generality, the expression has a form of

$$\dot{\mathbf{x}}(t) = \mathbf{A}\mathbf{x}(t) + \mathbf{B}\mathbf{u}(t) + \mathbf{F}\Delta\mathbf{P}(t) \tag{3}$$

Consider the parameter uncertainties and the modelling errors. (3) can be written by

$$\dot{\mathbf{x}}(t) = (\mathbf{A}' + \Delta\mathbf{A})\,\mathbf{x}(t) + (\mathbf{B}' + \Delta\mathbf{B})\,\mathbf{u}(t) + (\mathbf{F}' + \Delta\mathbf{F})\,\Delta\mathbf{P}(t) \tag{4}$$

Here $\mathbf{A}'$, $\mathbf{B}'$ and $\mathbf{F}'$ denote the nominal constant matrices, $\Delta\mathbf{A}\mathbf{x}(t)$, $\Delta\mathbf{B}\mathbf{u}(t)$ and $\Delta\mathbf{F}\Delta\mathbf{P}(t)$ denote the parameter uncertainties and the modelling errors.

Power systems actually cover the GRC nonlinearity. The existence of GRC has adverse effects on the system stability. Inherently, the GRC nonlinearity acts as a limiter to limit the rate of change in the generating power. From Figure 1, such a nonlinear power system can be formulated by

$$\dot{\mathbf{x}}(t) = \mathbf{A}'\mathbf{x}(t) + \mathbf{B}'\mathbf{u}(t) + \mathbf{F}'\Delta\mathbf{P}(t) + \Delta\mathbf{A}\mathbf{x}(t) + \Delta\mathbf{B}\mathbf{u}(t) + \Delta\mathbf{F}\Delta\mathbf{P}(t) + \phi(t) \tag{5}$$

where $\phi(t)$ denotes the uncertainties due to the GRC nonlinearity.

From (5), the LFC design of the nonlinear power system with wind turbines can be divided into two parts. One is to design a controller for the nominal system. The other is to consider how to suppress the system uncertainties.

3. **Control Design.**

3.1. **Design of sliding mode control.** Assume that $||\mathbf{d}(t)|| \le d_0$, where $||\cdot||$ denotes the Euclidean norm, d_0 is constant but unknown and $\mathbf{d}(t)$ lumps all the uncertain terms in (5), determined by $\mathbf{d}(t) = F'\Delta\mathbf{P}(t) + \Delta\mathbf{A}\mathbf{x}(t) + \Delta\mathbf{B}\mathbf{u}(t) + \Delta\mathbf{F}\Delta\mathbf{P}(t) + \phi(t)$. Note that $\mathbf{d}(t)$ is unmatched. In order to develop a sliding mode controller for the LFC problem of such an uncertain power system (5), the sliding surface (6) is defined by

$$\mathbf{s} = \mathbf{c}^T\mathbf{x} \tag{6}$$

where $\mathbf{c}$ is a sliding-surface parameter vector.

Invented by V. I. Utkin [10], the SMC law is composed of two components. One is equivalent control law and the other is switching control law. In order to obtain the equivalent control law, we differentiate $\mathbf{s}$ in (6) with respect to t. Then, substituting (5) into $\dot{\mathbf{s}}$ yields

$$\dot{\mathbf{s}} = \mathbf{c}^T\dot{\mathbf{x}} = \mathbf{c}^T\mathbf{A}'\mathbf{x}(t) + \mathbf{c}^T\mathbf{B}'\mathbf{u}(t) + \mathbf{c}^T\mathbf{d}(t) \tag{7}$$

When the system trajectory enters the sliding mode stage and keeps on the sliding surface [10], the equivalent control law of the SMC system can be deduced from (7).

$$\mathbf{u}_{eq}(t) = -\left(\mathbf{c}^T\mathbf{B}'\right)^{-1}\mathbf{c}^T\mathbf{A}'\mathbf{x} - \left(\mathbf{c}^T\mathbf{B}'\right)^{-1}\mathbf{c}^T\mathbf{d}(t) \tag{8}$$

Owing to the effects of uncertainties, the system trajectory cannot keep on sliding along the sliding surface (6) perfectly. To attack the issue, the reachability condition of SMC [10] is taken into consideration, described by $\frac{\mathbf{s}^T\dot{\mathbf{s}}}{||\mathbf{s}||} < 0$. Here $\|\cdot\|$ means 2-norm. Substituting (7) into the left side of the reachability condition yields

$$\frac{\mathbf{s}^T\dot{\mathbf{s}}}{||\mathbf{s}||} = \frac{\mathbf{s}^T}{||\mathbf{s}||}\left[\mathbf{c}^T\mathbf{A}'\mathbf{x}(t) + \mathbf{c}^T\mathbf{B}'\mathbf{u}(t) + \mathbf{c}^T\mathbf{d}(t)\right] \tag{9}$$

In order that the reachability condition holds true, the SMC law can be defined by

$$\mathbf{u}(t) = -\left(\mathbf{c}^T\mathbf{B}'\right)^{-1}\mathbf{c}^T\mathbf{A}'\mathbf{x} - \left(\mathbf{c}^T\mathbf{B}'\right)^{-1}||\mathbf{c}||\bar{\mathbf{d}}_0 - \left(\mathbf{c}^T\mathbf{B}'\right)^{-1}\left[\eta\,\mathrm{sgn}(\mathbf{s}) + \kappa\mathbf{s}\right] \tag{10}$$

where $\bar{\mathbf{d}}_0 = \bar{d}_0\,\mathrm{sgn}(\mathbf{s})$, $\mathrm{sgn}(\mathbf{s})$ is a signum function vector, scalar parameters η and κ are positive constants.

Since $\bar{d}_0$ exists in (10), the value of $\bar{d}_0$ must be known to guarantee the system stability. Unfortunately, the boundary value is rather difficult to know in practice. In the aforementioned assumption, the uncertainties have an unknown boundary in the LFC system. Consequently, how to deal with the issue has to be considered.

3.2. **Design of RBF neural networks.** RBF neural networks can directly map from input-output data with a simple topological structure, which are powerful to approximate complex nonlinearities. In order to fill this gap between the guaranteed system stability and the unknown boundary value, RBF neural networks are employed.

Concerning the mathematical model (5), each element in $\mathbf{x}$ is employed as an input element. Accordingly, the network output y is defined as the estimated boundary value of the system uncertainties. Illustrated in Figure 3, the designed RBF neural networks contain m inputs, 1 output and l neurons in the hidden layer, where m is the dimension of $\mathbf{x}$ and l is the number of neurons in the hidden layer.

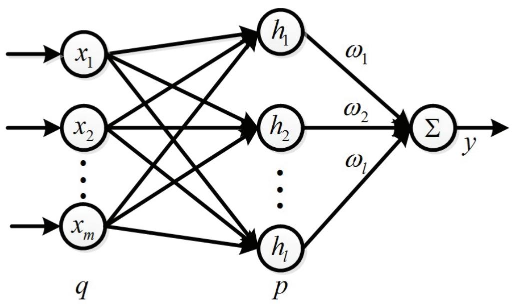

FIGURE 3. Structure of RBF networks

From Figure 3, define $y = \hat{\bar{d}}_0(\mathbf{x}, \omega)$. Then, the network output can be calculated by

$$\hat{\bar{d}}_0(\mathbf{x}, \omega) = \omega^T\mathbf{h}(\mathbf{x}) \tag{11}$$

where $\omega \in \mathscr{R}^l$ is the weight vector of the RBF networks. $\mathbf{h}(\mathbf{x}) \in \mathscr{R}^l$ is the Gaussian function vector and the pth element $h_p(\mathbf{x})$ of the vector $\mathbf{h}(\mathbf{x})$ is defined by

$$h_p(\mathbf{x}) = \exp\left[-\|\mathbf{x} - \mathbf{c}_p\|^2/(2b_p^2)\right] \tag{12}$$

where $p = 1, 2, \ldots, l$. $\mathbf{c}_p \in \mathscr{R}^m$ is the center vector of the pth Gaussian function. b_p is scalar, indicating the width of the pth Gaussian function. Both $\mathbf{c}_p$ and b_p are predefined.

Define $\hat{\bar{\mathbf{d}}}_0 = \hat{\bar{d}}_0 \operatorname{sgn}(\mathbf{s})$. Then, the SMC law (10) can be rearranged by

$$\mathbf{u}(t) = -\left(\mathbf{c}^T\mathbf{B}'\right)^{-1}\mathbf{c}^T\mathbf{A}'\mathbf{x} - \left(\mathbf{c}^T\mathbf{B}'\right)^{-1}||\mathbf{c}||\hat{\bar{\mathbf{d}}}_0 - \left(\mathbf{c}^T\mathbf{B}'\right)^{-1}[\eta \operatorname{sgn}(\mathbf{s}) + \kappa\mathbf{s}] \tag{13}$$

3.3. **Stability analysis.** In (11), ω has to be renewed by an update law in order that $\hat{\bar{d}}_0$ can match the change of uncertainties. Since the update law makes a difference to the system stability, this topic should be investigated in the sense of Lyapunov.

Assumption 1: There is an optimal weight ω^* such that $\left|\omega^{*T}\mathbf{h}(\mathbf{x}) - \bar{d}_0\right| = \varepsilon(\mathbf{x}) < \varepsilon_1$.

Assumption 2: There is ε_0 such that $\bar{d}_0 - \|\mathbf{d}(t)\| > \varepsilon_0 > \varepsilon_1$.

Theorem 3.1. *Take Assumptions 1 and 2 into account. Consider the uniform system (5), define the sliding surface (6) and adopt the SMC law (13). Then, the SMC-based LFC system is of asymptotical stability if the update law of ω has a form of*

$$\dot{\omega} = \xi\|\mathbf{s}\|_1\|\mathbf{c}\|\mathbf{h}(\mathbf{x}) \tag{14}$$

where $\xi = \|\mathbf{c}\|(\varepsilon_0 - \varepsilon_1)$ is a positive constant and $\|\cdot\|_1$ means 1-norm.

Proof: Consider the following Lyapunov function candidate

$$V = \left(\mathbf{s}^T\mathbf{s} + \xi^{-1}\tilde{\omega}^T\tilde{\omega}\right)/2 \tag{15}$$

where $\tilde{\omega}$ is determined by $\tilde{\omega} = \omega^* - \omega$.

Differentiate V with respect to time t in (15) and substitute $\tilde{\omega} = \omega^* - \omega$ into the derivative of V. The derivative of V can be formulated by

$$\dot{V} = \mathbf{s}^T\dot{\mathbf{s}} - \xi^{-1}\tilde{\omega}^T\dot{\omega} \tag{16}$$

In (16), replace $\dot{\mathbf{s}}$ by (7) and consider the SMC law (13). Then, (16) becomes

$$\begin{aligned}\dot{V} &= \mathbf{s}^T\dot{\mathbf{s}} - \xi^{-1}\tilde{\omega}^T\dot{\omega} = \mathbf{s}^T\left[\mathbf{c}^T\mathbf{A}'\mathbf{x}(t) + \mathbf{c}^T\mathbf{B}'\mathbf{u}(t) + \mathbf{c}^T\mathbf{d}(t)\right] - \xi^{-1}\tilde{\omega}^T\dot{\omega}\\ &= \mathbf{s}^T\left[-\eta \operatorname{sgn}(\mathbf{s}) - \kappa\mathbf{s} - ||\mathbf{c}||\hat{\bar{\mathbf{d}}}_0 + \mathbf{c}^T\mathbf{d}(t)\right] - \xi^{-1}\tilde{\omega}^T\dot{\omega}\\ &\leqslant \left(-\eta\|\mathbf{s}\|_1 - \kappa\|\mathbf{s}\|^2\right) - \|\mathbf{s}\|_1||\mathbf{c}||\left(\hat{\bar{d}}_0 - \bar{d}_0\right) - \|\mathbf{s}\|_1||\mathbf{c}||\left(\bar{d}_0 - \|\mathbf{d}(t)\|\right) - \xi^{-1}\tilde{\omega}^T\dot{\omega}\end{aligned} \tag{17}$$

Substituting (11) and (14) into (17) yields

$$\dot{V} \leqslant \left(-\eta\|\mathbf{s}\|_1 - \kappa\|\mathbf{s}\|^2\right) + \|\mathbf{s}\|_1||\mathbf{c}||\left[|\varepsilon(\mathbf{x})| - \left(\bar{d}_0 - \|\mathbf{d}(t)\|\right)\right] \tag{18}$$

From Assumptions 1 and 2, $|\varepsilon(\mathbf{x})| - \left(\bar{d}_0 - \|\mathbf{d}(t)\|\right) < \varepsilon_1 - \varepsilon_0$ such that $\dot{V} < 0$ in (18). In the sense of Lyapunov, the SMC-based LFC system is asymptotically stable. □

4. **Simulation Results.** An interconnected power system with wind turbines is utilized to verify the proposed scheme. The power system consists of two control areas. Each control area has an aggregated generating unit with GRC in Figure 1 and an aggregated wind turbine unit in Figure 2. The system schematic is illustrated in Figure 4. Concerning the renewable power system, all physical parameters are presented in [3].

Consider the SMC controllers. Their sliding surfaces are determined by Acker command of MATLAB. Other parameters of the four controllers are set by $\eta = 0.1$ and $\kappa = 10$. Concerning the RBF NNs, the initial weights between the hidden and output layers are set by random numbers in the open interval $(0, 1)$ as well as the widths of the Gaussian function vectors. Other parameters of the networks are set by $\xi_0 = 0.002$ and $\xi_1 = 0.001$.

To show the performance of the presented method, two step load disturbances $P_{L1} = P_{L2} = 1\%$ are simultaneously applied to the interconnected power system at $t = 5$s. Figure 5 illustrates the frequency deviations, the area control errors, the deviations of tie-line active power and the outputs of the four RBF NNs. Without doubt, the system state changes of the LFC system with RBF NNs in Figure 5 are smoother and the settling times are shorter.

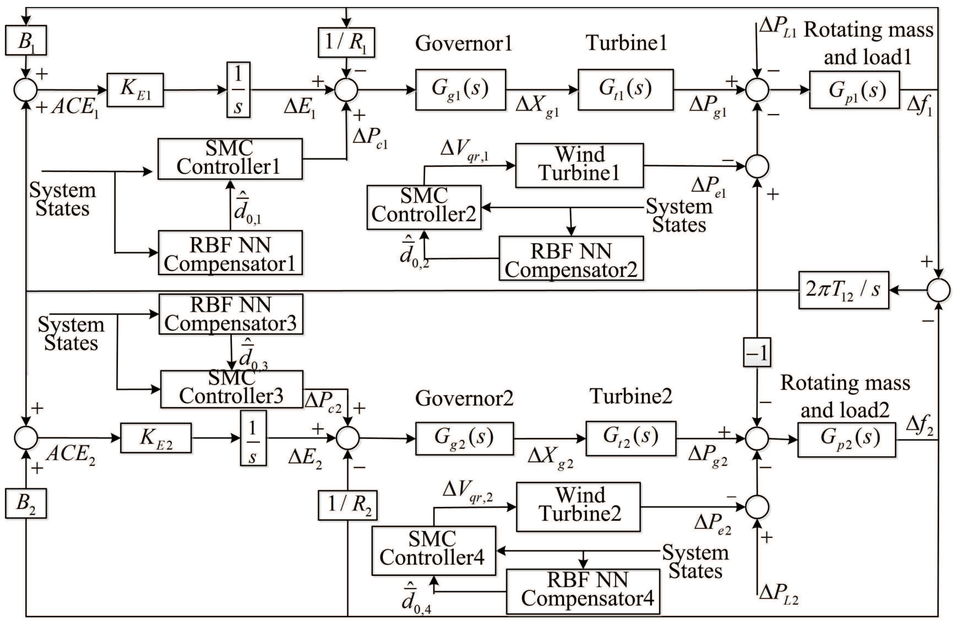

FIGURE 4. Block diagram of the considered two-area power system

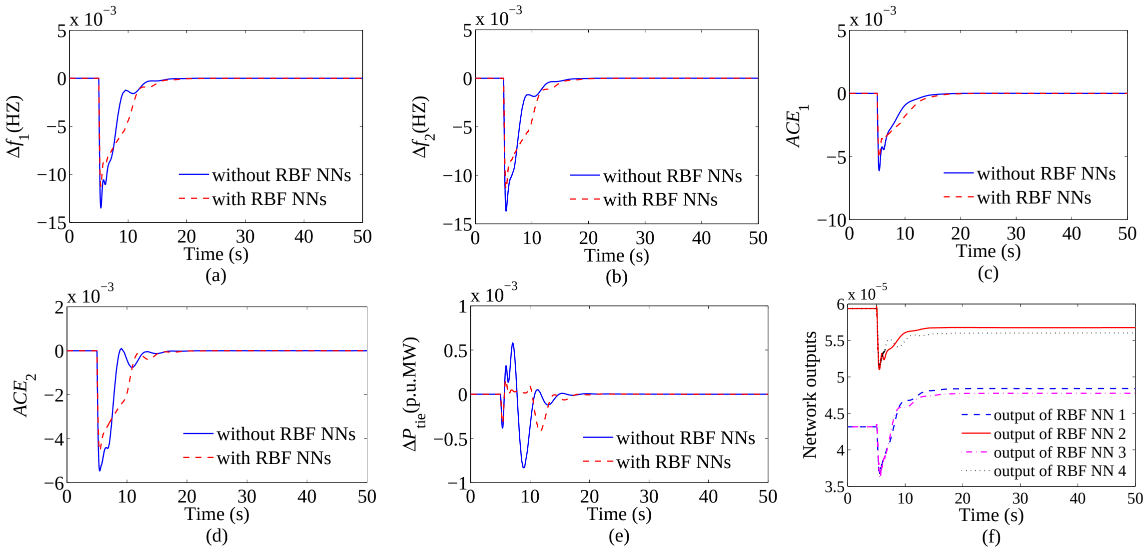

FIGURE 5. Simulation results: (a) Δf_1; (b) Δf_2; (c) ACE_1; (d) ACE_2; (e) ΔP_{tie}; (f) RBF NNs outputs in the two control areas

5. **Conclusions.** This article has addressed the LFC problem for renewable power systems in the presence of GRC. The control scheme is by means of SMC. To suppress the uncertainties of the LFC problem, RBF networks are adopted. The theoretical analysis proves that the SMC-based LFC system is of asymptotic stability. The presented control scheme has achieved the LFC problem of an interconnected renewable power system. How to apply the proposed method to an integrated wind/solar system would constitute an important area for future research.

Acknowledgment. This work is supported by the China Three Gorges New Energy Co. Ltd. and the Fundamental Research Funds for the Central Universities under Grant No. 2015MS29.

REFERENCES

[1] W. Jiang, J. Lu and Y. Mei, Study on frequency control strategy of wind farm-energy storage system, *ICIC Express Letters*, vol.9, no.10, pp.2657-2663, 2015.
[2] S. Alshibani, V. G. Agelidis and R. Dutta, Lifetime cost assessment of permanent magnet synchronous generators for MW level wind turbines, *IEEE Trans. Sustainable Energy*, vol.5, no.1, pp.10-17, 2014.
[3] T. Mohamed, J. Morel, H. Bevrani and T. Hiyama, Model predictive based load frequency control-design concerning wind turbines, *International Journal of Electrical Power and Energy Systems*, vol.43, no.1, pp.859-867, 2012.
[4] D. W. Qian, D. B. Zhao, J. Q. Yi and X. J. Liu, Neural sliding-mode load frequency controller design of power systems, *Neural Computing and Applications*, vol.22, no.2, pp.279-286, 2013.
[5] Y. Mi, Y. Fu, C. Wang and P. Wang, Decentralized sliding mode load frequency control for multi-area power systems, *IEEE Trans. Power Systems*, vol.28, no.4, pp.4301-4309, 2013.
[6] Z. Al-Hamouz, H. Al-Duwaish and N. Al-Musabi, Optimal design of a sliding mode AGC controller: Application to a nonlinear interconnected model, *Electric Power Systems Research*, vol.81, no.7, pp.1403-1409, 2011.
[7] K. Vrdoljak, N. Peric and I. Petrovic, Sliding mode based load-frequency control in power systems, *Electric Power Systems Research*, vol.80, no.5, pp.514-527, 2010.
[8] D. Qian, J. Yi and X. Liu, Sliding mode technology for automatic generation control of single area power systems, *ICIC Express Letters*, vol.5, no.8(A), pp.2415-2421, 2011.
[9] R. Selmic and F. Lewis, Neural-network approximation of piecewise continuous functions: Application to friction compensation, *IEEE Trans. Neural Networks*, vol.13, no.3, pp.745-751, 2002.
[10] V. I. Utkin, *Sliding Modes in Control and Optimization*, Springer-Verlag, Berlin, 1992.